Title

Selective Reduction of Nitroarenes via Noncontact Hydrogenation

Journal

Journal of the American Chemical Society, 146(43)

ISSN

0002-7863

Authors

An, Hua
Ding, Yani
Sautet, Philippe
et al.

Publication Date

2024-10-30

DOI

10.1021/jacs.4c06011

Selective reduction of nitroarenes via non-contact hydrogenation

Hua An[1,2], Yani Ding[2], Philippe Sautet[4,5], Geng Sun[6,*] and Ning Yan[1,2,3,*]

[1]Joint School of National University of Singapore and Tianjin University, International Campus of Tianjin University, Binhai New City, Fuzhou 350207, China.

[2]Department of Chemical and Biomolecular Engineering, National University of Singapore, Singapore 117585, Singapore.

[3]Centre for Hydrogen Innovations, National University of Singapore, Singapore 117580, Singapore

[4]Department of Chemical and Biomolecular Engineering, University of California, Los Angeles, Los Angeles, California 90095, USA.

[5]Department of Chemistry and Biochemistry, University of California, Los Angeles, Los Angeles, California 90095, USA.

[6]School of Chemistry and Chemical Engineering, Chongqing University, Chongqing 401331, China.

ABSTRACT: In traditional hydrogenation, where H_2 and substrates with unsaturated bonds are activated on the same catalyst (contact mode), competitive hydrogenation of multiple reducible groups often occurs. We introduce a non-contact hydrogenation method for selective reduction of the nitro group when multiple reducible groups are present. The set-up is based on an unbiased H-cell that spatially separates H_2 and nitroarenes into two chambers connected by a proton-exchange membrane, thus effectively decoupling the steps of H_2 activation and reduction of unsaturated groups. Through a unique proton/electron transfer pathway that is specific to nitro functional group reduction to hydroxylamine, side reactions like C=C, C=O, and C≡C bond hydrogenation are fully avoided. Utilizing commercial Pd/C for H_2 activation and carbon nanotubes for proton/electron transfer, we achieve 100% nitro-group reduction selectivity in hydrogenation of a series of nitroarenes, in sharp contrast to negligible selectivity over the same catalysts in a batch reactor under contact mode. This non-contact approach offers a strategy for enhancing selectivity in hydrogenation reactions, moving beyond the traditional focus on catalyst active site engineering.

INTRODUCTION

The selective catalytic hydrogenation of nitroarenes possessing multiple reducible groups into nitroso, azoxy, hydroxylamines, and amines constitutes a critical chemical process extensively utilized across various sectors, including the dye, pharmaceutical, and food industries.[1-6] Typically, the hydrogenation process involves co-feed H_2 and nitroarenes in a single reactor where they are activated on the same catalyst surface, referred to as contact hydrogenation (i.e., H_2 and nitroarenes are under contact with each other).[7-10] However, the reaction often leads to the competitive reduction of undesired reducible groups. To address this issue, significant research efforts have been dedicated to developing catalysts to improve selectivity guided by the Langmuir-Hinshelwood (L-H) mechanism,[11-15] which suggests that hydrogenation performance is largely determined by the interaction between co-adsorbed hydrogen atoms and unsaturated functional groups on adjacent sites.[16-21] A common strategy is to fine-tune the active sites to favor the adsorption of the nitro group ($-NO_2$) over other unsaturated groups such as C≡C, C=C, -CHO, and -X (X = Cl, Br, I) either by electronic or geometric modifications.[22-25]

On the other hand, it has been demonstrated that nitro group hydrogenation can proceed via a non-L-H mechanism, namely through a proton-electron addition pathway, including the decomposition of hydrogen into electrons and protons at active sites, followed by the direct reduction of the nitro group through electron capture from the catalyst surface and protons from protic solvents.[26-32] Such a mechanism removes the need for $-NO_2$ and H atoms to be co-adsorbed on the same catalyst surface, paving the way for catalytic systems that facilitate selective hydrogenation of $-NO_2$ group via the proton-electron addition while leaving other functional groups unaffected. Along this line, thiol molecules have been introduced to cover the Pt, Pd or Ni catalyst surface, limiting the co-adsorption of H and the substrate, and thus enhancing selective hydrogenation.[33-36]

While the catalyst development will continue to play a crucial role to the field, there also exists an underexplored opportunity in achieving high selectivity without the design of new catalysts: tailored engineering of catalytic reactors to favor the proton-electron addition pathway. Compared with designing catalysts with elegantly controlled structure, this approach would circumvent the challenges of scalability, reproducibility and/or costs often associated with new catalyst development.

Recognizing this potential, we introduce a non-contact hydrogenation process aimed at selectively reducing $-NO_2$ groups using common and commercially available materials. Via physically separating H_2 and substrates across the anode and cathode of H-type electrochemical cell (H-cell), our non-contact hydrogenation process effectively restricts unnecessary hydrogen-substrate interaction that leads to

non-selective hydrogenation. With Pd as the anode for H_2 oxidation and carbon nanotubes (CNTs) as the cathode for -NO_2 reduction, this configuration enables the selective hydrogenation of nitroarenes with multiple reducible groups, such as C=C, C≡C and -CHO, into primary hydroxylamines. Contrastingly, traditional single cell set-up (S-cells) that co-feed H_2 and substrates into one chamber exhibits negligible selectivity towards primary hydroxylamines using the same catalyst. Our mechanistic study elucidates that nitro groups are directly reduced to -NHOH by capturing electrons and protons from the CNT surface and protonic solvent, respectively, via an out-sphere electron transfer mechanism. This mechanism eliminates the presence of adsorbed hydrogen atom on catalyst surface which is essential for the hydrogenation of C=C, C≡C, and -CHO bonds via L-H mechanism.

RESULTS AND DISCUSSION

In conventional contact hydrogenation, H_2 is dissociated into hydrogen atoms upon interaction with noble metal surfaces, such as Pd. This subsequently leads to the non-selective reduction of various unsaturated functional groups, including C≡C and C=C bonds, as well as aldehyde (-CHO) and nitro (-NO_2) groups, on the same metal catalyst surface (Figure 1Ai). To illustrate this phenomenon, and for comparison purpose later, we employed an electrochemical single cell (S-cell) to represent traditional liquid-phase thermal hydrogenation using PdC as the catalyst. This setup co-fed hydrogen and various substrates, such as ethenylbenzene, phenylacetylene, benzaldehyde, and nitrobenzene, into the same cell. As displayed in Figure 1Aii and Aiii, all four types of unsaturated functional groups were completely reduced to their saturated counterparts, exemplifying the lack of selectivity in traditional hydrogenation when a common commercial catalyst such as PdC was used.

Subsequently, we explored the non-contact hydrogenation of nitroarenes using an H-cell, in which H_2 and substrates were separately supplied to the anode chamber and the cathode chamber, respectively. As such, the reaction is divided into two distinct electrochemical half-reactions: the oxidation of H_2 to protons and electrons at the anode and the reduction of substrates through the acquisition of protons and electrons at the cathode (Figure 1Bi). Initially, we conducted a confirmatory experiment employing PdC for the H_2 oxidation and doped carbon nanotubes (CNTs) on carbon paper for the reduction reactions at the cathode. As demonstrated in Figure 1Bii and 1Biii, and further detailed in Figure S1, the current within the H-cell remained negligible upon sequential addition of phenylacetylene, ethenylbenzene, and benzaldehyde, indicating no product formation. However, when nitrobenzene was introduced to the cathode chamber, there was a significant increase in current, together with the detection of N-hydroxyaniline and aniline reduction products at the cathode, thereby highlighting the exceptional selectivity of the setup towards -NO_2 reduction.

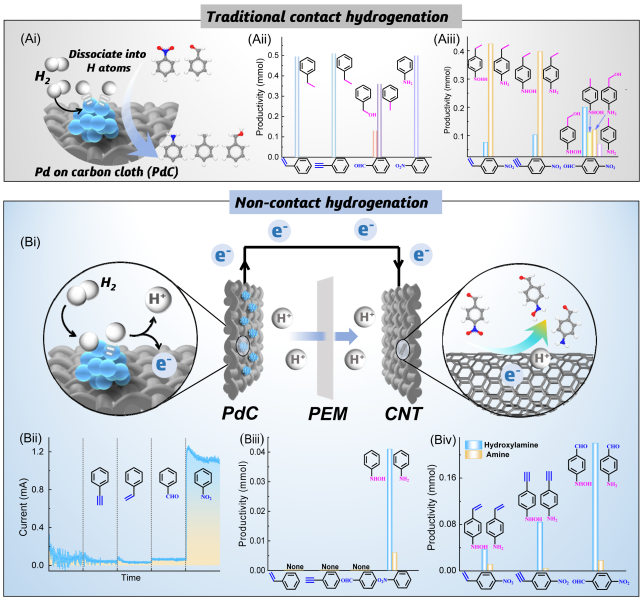

Figure 1. (Ai) Traditional contact hydrogenation using PdC (5 wt.%) in a single electrochemical cell (S-cell), (Aii) and (Aiii) Product distribution of ethenylbenzene, phenylacetylene, benzaldehyde, nitrobenzene, 4-nitrostyrene, 4-ethynylnitrobenzene and 4-nitrobenzaldehyde hydrogenation via the contact mode in the S-cell, (Bi) Non-contact hydrogenation in a H-type electrochemical cell (H-cell) with PdC (5 wt.%) as anode for hydrogen oxidation and CNT as the cathode for the reduction reaction, (Bii) Current for the H-cell with sequential addition of phenylacetylene, ethenylbenzene, benzaldehyde and nitrobenzene, (Biii) and (Biv) Product distribution of ethenylbenzene, phenylacetylene, benzaldehyde, nitrobenzene, 4-nitrostyrene, 4-ethynylnitrobenzene and 4-nitrobenzaldehyde hydrogenation via the non-contact mode in the H-cell. All experiments were conducted in 50 vol. % acetonitrile and 50 vol. % aqueous solution of H_2SO_4 (1 M) mixture electrolyte for cathode side and aqueous solution of H_2SO_4 (1 M) for anode side.

Next, by using this H-cell setup we proceeded to evaluate the selective hydrogenation of several substrates containing various unsaturated functional groups, including 4-nitrostyrene, 4-ethynylnitrobenzene, and 4-nitrobenzaldehyde. As shown in Figure 1Biii (further details provided in Figure S2), the nitro groups were selectively reduced to primary hydroxylamino (-NHOH) together with a minor fraction of amino (-NH_2) functionalities while completely preserving the para-group C≡C, C=C, or -CHO functionalities. Interestingly, the hydrogenation activity increased with the electron-withdrawing capability of the substituent at the para position. This suggests that a reduced electron density on the benzene ring facilitates the nitro group's electron capture from the electrode surface, aligning with the electron transfer nature of the reaction. Based on these experiments, it is established that the non-contact hydrogenation methodology offers high selectivity for reducing nitroarenes that concurrently bear multiple reducible functional groups.

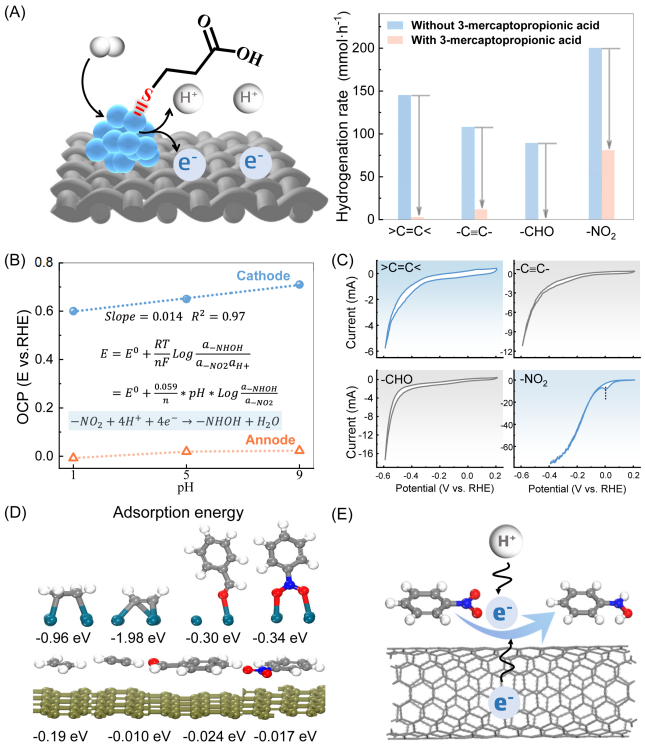

Figure 2. (A) (left) A diagram illustrating the active site poisoning experiment at the cathode side of the H-cell with PdC (5 wt. %) electrode and (right) hydrogenation rate comparison of ethylene, propiolic acid, 4-hydroxybenzaldehyde and 4-nitrobenzenesulfonic acid hydrogenation without and with the addition of 20 μL 3-mercaptopropionic acid in pH 1 electrolyte, (B) Open-circuit potential of the cathode with respect to pH for 4-nitrobenzenesulfonic acid hydrogenation over the PdC (5 wt.%) electrode for hydrogen oxidation and CNT for the reduction reaction in H-cell, (C) Cyclic voltammetry (CV) curve of ethylene, propiolic acid, 4-hydroxybenzaldehyde and 4-nitrobenzenesulfonic acid hydrogenation over CNT electrode in a pH 1 electrolyte in S-cell, (D) Adsorption energy of the C=C double bond, C≡C triple bond, -CHO and -NO_2 on Pd(111) and on the carbon surface via DFT calculation, and (E) A diagram illustrating the non-contact hydrogenation of -NO_2 to -NHOH in the cathode.

We further conducted non-contact hydrogenation of ethylene (C=C bond), propiolic acid (C≡C bond), 4-hydroxybenzaldehyde (C=O bond), and 4-nitrobenzenesulfonic acid (-NO_2) employing PdC or PtC at both the anode and cathode. The purpose is to systematically compare the catalytic performances under non-contact (in the H-cell) and contact (in the S-cell) hydrogenation modes across a wide pH range of 1-13. These experiments were conducted in kinetic regions with negligible hydrogen mass transfer limitations (Figure S3). Activity and selectivity findings are compiled in Figure S8, with detailed product analyses available in Figures S4-S7. Not unexpected, hydrogenation products were detected for all four substrates in both modes. Importantly, the selectivity to acrylic acid and 4-hydroxybenzyl alcohol remained consistent in two reactor setups, suggesting identical reaction pathways under both contact and non-contact hydrogenation modes. However, selectivity towards 4-(hydroxyamino)benzenesulfonic acid during 4-nitrobenzenesulfonic acid hydrogenation in the H-cell was significantly higher than that in the S-cell, indicating a contact-mode-dependent mechanism for -NO_2 group reduction compared to the other functional groups. These data suggests that the L-H mechanism predominates for C=C, C≡C, and C=O bond hydrogenations for both contact and non-contact hydrogenation. For the latter (non-contact hydrogenation), the combination of protons and electrons to form surface-adsorbed hydrogen atoms is required. Thus, this hydrogenation pathway can be blocked in non-contact hydrogenation if cathode is not able to convert proton and electron to surface hydrogen. On the other hand, the -NO_2 group reduction plausibly follow both L-H and proton-electron addition pathways, with the latter becoming more prevalent in the non-contact mode.

To confirm this, 3-mercaptopropionic acid (MPA), known for its strong binding that block Pd active sites,[37-40] was added to the PdC electrode in the cathode chamber in non-contact hydrogenation. Indeed, a notable decline in reaction rates for ethylene and propiolic acid hydrogenation were detected following MPA addition (Figures 2A and S9), while a full deactivation was observed for 4-hydroxybenzaldehyde hydrogenation. In sharp contrast, approximately 50% of the initial activity for 4-nitrobenzenesulfonic acid hydrogenation persisted. Even when PdC was replaced by Pd plate, about 25% activity remained (Figure S10). After poisoning the PdC electrode, the only product is 4-(hydroxyamino)benzenesulfonic acid, which is a four-electron reduction product of -NO_2.

Subsequent open-circuit potential (OCP) tests were conducted under varying pH conditions using an Ag/AgCl reference electrode, aiming to further elucidate half-reactions under the non-contact hydrogenation mode. PdC and CNT were used for the anode and cathode, respectively (Figures 2B and S12). For ethylene, propiolic acid, and 4-hydroxybenzaldehyde hydrogenation, the pH-OCP curve slopes were approximately 0.29 mV•pH^{-1}, suggesting that the possible cathode reaction is a two-electron reduction reaction according to the Nernst equation.[41-45] In stark contrast, the slope for 4-nitrobenzenesulfonic acid hydrogenation approximated 14.8 mV•pH^{-1}, indicating a four-electron reduction on the CNT surface, corroborating the activity test results where hydroxylamine was predominated. These findings further align with cyclic voltammetry (CV) outcomes using a CNT electrode under a nitrogen atmosphere in the S-cell (Figure 2C), where a reduction peak near zero potential (vs. RHE) was observed for 4-nitrobenzenesulfonic acid due to electron consumption. No such feature was observed in the presence of other functional groups.

Then we analyzed the geometric configuration and adsorption energy of the C=C, C≡C, -CHO and -NO_2 groups on Pd(111) surface and on the carbon surface via DFT calculations (Figure 2D). The four functional groups would tightly chemisorb on the Pd surface and form chemical bonds with Pd atoms, while they would physisorb on the carbon surface with a distance around 3 Å from molecules to the carbon surface. Consequently, the four-electron reduction of -NO_2 to -NHOH on CNT surface depends on the outer sphere electron transfer without the chemisorption of -NO_2 (Figure 2E).

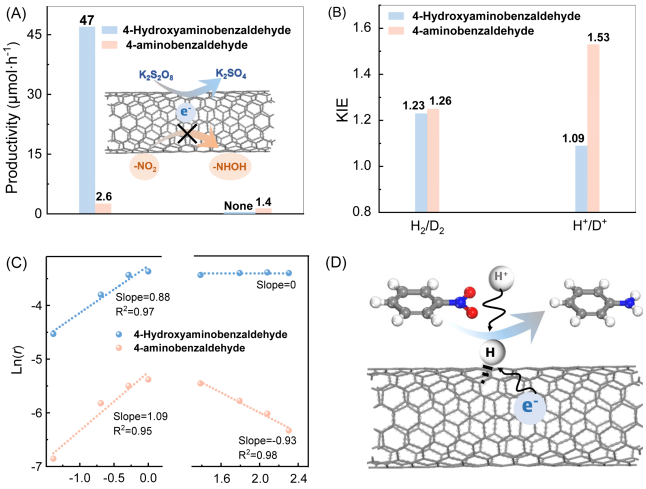

Figure 3. (A) Reaction rate change of 4-nitrobenzaldehyde hydrogenation to 4-(hydroxyamino)benzaldehyde and 4-aminobenzaldehyde without and with the addition of $K_2S_2O_8$ as electron scavenger at the cathode side of H-cell using CNT as cathode and PdC (5 wt. %) as anode, (B) Isotope effect of 4-nitrobenzaldehyde hydrogenation and (C) Reaction order of hydrogen and 4-nitrobenzaldehyde using PdC (0.04 wt. %) electrode for hydrogen oxidation and CNT for the reduction reaction in the H-cell and (D) A diagram illustrating the hydrogenation of -NO_2 to -NH_2 in the cathode.

It is noteworthy that the selectivity of -NO_2 hydrogenation differs markedly between contact and non-contact modes. In contact hydrogenation when PdC is used as the catalyst, the primary product is the amine (-NH_2). Conversely, in non-contact hydrogenation, with PdC as the anode and carbon nanotubes (CNT) as the cathode, hydroxylamine (-NHOH) predominates, with only a minor fraction of amine product. This discrepancy suggests disparate reaction pathways for the formation of amine and hydroxylamine. To validate this, we carried out non-contact hydrogenation tests using 4-nitrobenzaldehyde as the substrate, with PdC as anode and CNT as cathode within the H-cell. Adding $K_2S_2O_8$ as an electron scavenger into the H-cell cathode chamber entirely inhibited the production of 4-(hydroxyl)aminobenzaldehyde (Figures 3A and S13), while retaining over 50% activity for 4-aminobenzaldehyde formation. This demonstrates that the conversion of -NO_2 to -NHOH entirely relies on capturing electrons from surface, whereas the transition from -NO_2 to -NH_2 does not.

Further insights were gained from isotope experiments conducted within the H-cell under conditions where mass transfer limitations are eliminated (Figures 3B, S14, and S15). Replacing H^+ with D^+ at the cathode resulted in a kinetic isotope effect (KIE) of 1.09 for -NHOH formation, compared to 1.53 for -NH_2, suggesting that proton capture is not rate-determining for -NHOH synthesis but directly impacts -NH_2 formation. Meanwhile, substituting H_2 with D_2 at the anode similarly reduced the production rates of both -NH2 and -NHOH. Within this non-contact hydrogenation framework, the reaction orders for hydrogen in producing -NHOH and -NH_2 at the anode were 0.88 and 1.09, respectively, indicating similar dependency rates. Conversely, at the cathode, the reaction order was zero for 4-(hydroxyl)aminobenzaldehyde formation, but -0.93 for 4-aminobenzaldehyde (Figure 3C and S15), suggesting that high concentration of 4-nitrobenzaldehyde inhibits -NH_2 production but not -NHOH. These findings corroborate that -NHOH formation follows a distinct proton-electron transfer pathway, whereas -NH_2 synthesis follows the classical L-H mechanism. In the H-cell configuration, a small fraction of protons generates adsorbed hydrogen atoms on the CNT defect sites at the cathode, which then interact with -NO_2 to form -NH_2 (Figure 3D), in a similar way as reported on defect-containing graphene materials. [46, 47]

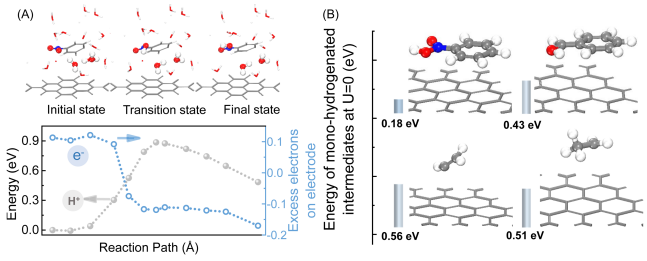

Figure 4. (A) Initial, transition and final state structure and energy profile for nitro hydrogenation via proton-electron addition (Only the nitro moiety, hydronium and a water molecule that assists the reaction are drawn with ball and stick models while other atoms are shown by sticks only.), and the potential energy profile is evaluated by the grand canonical DFT method fixing the electrode potential as approximately +0.6 eV (vs. SHE). (B) Stability of mono-hydrogenated products at U=0 vs. SHE evaluated using the computational hydrogen electrode method and implicit solvation. The red, white and blue balls are oxygen, hydrogen and nitrogen atoms respectively.

We conducted DFT calculations to analyze the reaction mechanism of nitro group hydrogenation on carbon electrode from a molecular perspective. The simulation exploits the grand canonical DFT method to control the electrode potential approximately at +0.6 eV (vs. SHE), being consistent with experiments. A single layer of graphene is exploited as the model for CNT cathode. Besides nitrobenzene, additional 16 water molecules are used as explicit water solvents. Implicit solvent is also located above the waters to screen the electrostatic field. The detailed theoretical setups are described in SI. In the initial structure (Figure 4A), both hydronium and nitrobenzene only physically interact with the carbon surface, with distances of around 5.4 Å and 4.4 Å from the nitro group and the hydronium to the electrode, and the electrode has approximately 0.1 excess electron per surface unit cell. During the reaction, a Grotthuss mechanism occurs: the hydronium donates a proton to the nearby water molecule which simultaneously gives a proton to the oxygen of nitro group, combined with 0.3 electrons transferred from the electrode to the reactant. The energy barrier between the initial and transition state is around 0.9 eV, and the energy of the final state is 0.49 eV higher than that of the initial state. The first hydrogen addition is probably the rate-determining step for -NO_2 to -NOHH, because the following steps are highly exothermic as seen in Figure S16. Therefore, the hydrogenation of -NO_2 could be accomplished via outer sphere electron transfer in solvent environment without the chemical adsorption from the theoretical viewpoint.

We also tried to explore the hydrogenation pathways for benzaldehyde, ethylene, and acetylene on the carbon electrode, but it is not possible to locate stable structures after

the first H atom addition (e.g. benzyl alcohol radical, ethyl, and vinyl) in the presence of electrode potential (+0.48 eV) and water environment. The structures of the proposed intermediates always dissociated into proton, electron and reactants spontaneously during the structure optimizations. Therefore, we evaluated the stabilities of the corresponding product radicals by the computational hydrogenation electrode method as displayed in Figure 4B. The first H atom hydrogenation of nitrobenzene is endothermic with energy about 0.18 eV at U=0 (vs. SHE), which increases to 0.66 eV at the experimentally measured potential (U=0.48 eV). In contrast, the energies of benzyl alcohol radical, ethyl, and vinyl are rather high, around 0.5 eV at U=0 and 1.0 eV at the working condition, which questions their stability and restricts their hydrogenation process on the carbon electrode. Their reactants or products weakly physisorb on the carbon surface at a distance larger than 3.0 Å. When comparing with the energies of intermediates without electrodes (Figure S17), this shows that the carbon electrode only acts as an electron conductor and does not change the stabilities of reactants/products.

For comparison, we investigated the hydrogenation of the aldehyde group on Pd surface with CH_2O as an example of substrates, as shown in Figure S18. Upon CH_2O hydrogenation reaction to form a new O-H bond, the electron-proton addition bears a low barrier, about 0.27 eV. The quenched structure of CH_2OH in water could not form stable hydrogen bond between hydrogen atoms and carbon atom of CH_2OH, therefore the formation of C-H bond via proton-electron addition has to undergo an unfavorable reorganization of the hydrogen bond network, leading to an extremely high energy barrier of 1.67 eV. As a comparison, the energy barriers are 0.65 and 1.01 eV for hydrogen atom addition to oxygen and carbon via surface L-H pathway. Hence, hydrogenation of the aldehyde group likely follows a hybrid mechanism, with the proton-electron addition to the oxygen and the H atom addition to the carbon.[48-50]

We evaluated the stability of the system for 4-nitrobenzaldehyde hydrogenation using 5 wt.% PdC and CNT as electrodes within the H-cell configuration. As displayed in Figure 5A, the production of 4-(hydroxyl)aminobenzaldehyde remained consistent after a 30-hour test without changing membrane or electrodes. On the other hand, the yield of the minor product, 4-aminobenzaldehyde, diminished after the second cycle, which may be attributed to the degradation of active sites. This observation aligns with the proposed mechanisms: outer sphere electron transfer mechanism for -NHOH generation and L-H pathway for $-NH_2$ production. From a practical perspective, this is intriguing since catalyst selectivity improves with repeated use. After the stability test, the morphology and structural quality of the CNT didn't change, as shown in Figure 5B.

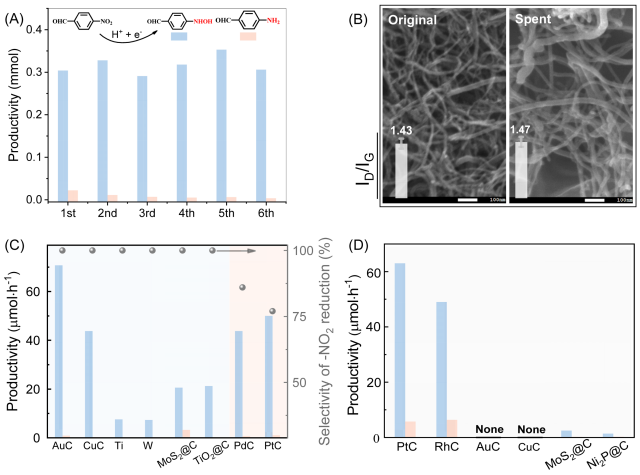

Figure 5. (A) Stability test for 4-nitrobenzaldehyde hydrogenation in the H-cell with PdC (5 wt.%) as anode and CNT as cathode, (B) SEM images and I_D/I_G values (The intensity ratio of the D and G bands, and a higher ratio ensures more defects) from Raman spectra of CNTs before and after the stability test, (C) Activity of different materials for the cathode side with PdC (5 wt.%) as anode and (D) Activity of different materials for the anode side with CNT as cathode for 4-nitrobenzaldehyde reduction in the H-cell. All experiments were conducted in 50 vol. % acetonitrile and 50 vol. % H_2SO_4 solution (1M) mixture electrolyte for cathode side and H_2SO_4 solution (1M) for anode side.

Based on the above mechanism studies, materials with good electron conductivity and poor chemisorption of $-NO_2$ would facilitate the selective reduction of $-NO_2$ via proton-electron addition. We further explored various conductors and semiconductors as cathode materials for nitro-group reduction while maintaining PdC as the anode for H_2 activation (Figure 5C and Figure S19). Indeed, Au, Cu, Ti, W, MoS_2 and TiO_2, in particular Au, show higher selectivity compared to that of Pd and Pt. On the anode side, the primary function is hydrogen oxidation into protons and electrons. Hence, materials effective in hydrogen activation, such as PtC, RhC, MoS_2, and NiP_2, exhibited satisfactory performance for $-NO_2$ hydrogenation in the H-cell with CNT as the cathode, with PtC showing the highest activity (Figure 5D and Figure S19).

These findings indicate that in non-contact hydrogenation, the activation of H_2 and substrates can be finely tuned independently. Further, the insights gained from these tests provide a rationale for the widespread use of Pt/Au bimetallic catalysts in $-NO_2$ hydrogenation[2,51-56] and provides an explanation why its activity is severely restricted in aprotic solvents[56-58]. Drawing from these results, we propose several guidelines for identifying suitable materials for the selective hydrogenation of nitroarenes via proton-electron addition, including effective hydrogen activation, poor chemisorption of $-NO_2$, excellent electron conductivity, and the use of protic solvents. These factors are beyond the scope of conventional approach in catalyst design.

CONCLUSION

In this study, we introduced and studied non-contact hydrogenation for the selective reduction of nitroarenes. By employing an H-cell configuration, we physically separated H_2 and substrates into distinct chambers, thereby decoupling H_2 activation from substrate reduction. This methodology

effectively eliminates the competitive hydrogenation typically observed with unsaturated bonds such as C≡C, C=C, and C=O, thus achieving complete functional group selectivity in the hydrogenation of various nitroarenes using commercially available PdC for H_2 activation and CNT for selective proton/electron transfer. Further mechanistic study highlights that -NO2 reduction to -NHOH is driven by an outer sphere electron transfer mechanism, which is the dominant pathway for non-contact hydrogenation that features much higher reaction barrier for other functional groups. Overall, our work provides a rare example of achieving selective hydrogenation avoiding the design of catalysts, and also offers insights into hydrogenation mechanisms of nitroarenes. Looking forward, non-contact hydrogenation allows for the independent optimization of H_2 activation and substrate reduction, which facilitates targeted catalyst customization.

ASSOCIATED CONTENT

Supporting Information.
Product quantification and current values of phenylacetylene, ethenylbenzene, benzaldehyde, nitrobenzene, 4-nitrobenzaldehyde, 1-ethynyl-4-nitrobenzene and 4-nitrostyrene hydrogenation hydrogenation via non-contact mode (Figure S1-2), product quantification and current values of ethylene, propiolic acid, 4-hydroxybenzaldehyde and 4-nitrobenzenesulfonic acid hydrogenation via contact and no-contact mode (Figure S3-8), poisoning experiment of ethylene, propiolic acid, 4-hydroxybenzaldehyde and 4-nitrobenzenesulfonic acid hydrogenation over PdC or Pd plate (Figure S9-10), OCP test of ethylene, propiolic acid, 4-hydroxybenzaldehyde and 4-nitrobenzenesulfonic acid hydrogenation over PdC and CNT (Figure S11-12), electron capture experiment, isotope experiment, and reaction order test of 4-nitrobenzaldehyde hydrogenation (Figure S13-15), free energy change of nitro group hydrogenation (Figure S16), stabilities of hydrogenated products after the first H atom addition in the absence of the graphene electrode (Figure S17), the energy barriers of CH_2O hydrogenation on Pd (111) surface (Figure S18), The activity of different materials for cathode side and anode side (Figure S19).

AUTHOR INFORMATION

Corresponding Author

*Email: sungengemail@cqu.edu.cn
*Email: ning.yan@nus.edu.sg

Author Contributions

N.Y. conceived and supervised the project. H.A conducted the experiments. N.Y., H.A. and G.S. analyzed the data and co-wrote the manuscript. H.A. and Y.D. draw the figures. G.S. performed DFT studies, and G.S. and P.S. analyzed the data. All authors discussed the results and edited the manuscript.

Notes

The authors declare no competing financial interest.

ACKNOWLEDGMENT

We thank the National Research Foundation, Singapore, NRF Investigatorship (NRFI07-2021-0015) for the financial support.

REFERENCES

(1) Formenti, D.; Ferretti, F.; Scharnagl, K. F.; Beller, M. Reduction of nitro compounds using 3d-non-noble metal catalysts. *Chem. Rev.* **2019**, *119*, 2611-2680.

(2) Corma, A.; Serna, P. Chemoselective hydrogenation of nitro compounds with supported gold catalysts. *Science* **2006**, *313*, 332-334.

(3) Zhang, L.; Zhou, M.; Wang, A.; Zhang, T. Selective hydrogenation over supported metal catalysts: from nanoparticles to single atoms. *Chem. Rev*. **2020**, *120* (2), 683-733.

(4) Lang, R.; Du, X.; Huang, Y.; Jiang, X.; Zhang, Q.; Guo, Y.; Liu, K.; Qiao, B.; Wang, A.; Zhang, T. Single-atom catalysts based on the metal-oxide interaction. *Chem. Rev.* **2020**, *120*, 11986-12043.

(5) Wang, D.; Astruc, D. The golden age of transfer hydrogenation. *Chem. Rev*. **2015**, *115* (13), 6621-6686.

(6) Yan H.; Zhao, X.; Guo, N.; Lyu, Z.; Du, Y.; Xi, S.; Guo, R.; Chen, C.; Chen, Z.; Liu, W.; Yao, C.; Li, J.; Pennycook, S. J.; Chen, W.; Su, C.; Zhang, C.; Lu, J. Atomic engineering of high-density isolated Co atoms on graphene with proximal-atom controlled reaction selectivity. *Nat. Commun*. **2018**, *9*, 1-9.

(7) Lara, P.; Philippot, K. The hydrogenation of nitroarenes mediated by platinum nanoparticles: an overview. *Catal. Sci. Technol.* **2014**, *4*, 2445-2465.

(8) Wang, L.; Guan, E.; Zhang, J.; Yang, J.; Zhu, Y.; Han, Y.; Yang, M.; Cen, C.; Fu, G.; Gates, B. C.; Xiao, F-S. Single-site catalyst promoters accelerate metal-catalyzed nitroarene hydrogenation. *Nat. Commun*. **2018**, *9*, 1362.

(9) Cai, S.; Duan, H.; Rong, H.; Wang, D.; Li, L.; He, W.; Li, Y. Highly active and selective catalysis of bimetallic Rh_3Ni_1 nanoparticles in the hydrogenation of nitroarenes. *ACS Catal*. **2013**, *3*, 608-612.

(10) Wang, L.; Zhang, J.; Wang, H.; Shao, Y.; Liu, X.; Wang, Y-Q.; Lewis, J. P.; Xiao, F-S. Activity and selectivity in nitroarene hydrogenation over Au nanoparticles on the edge/corner of anatase. ACS Catal. **2016**, *6*, 4110-4116.

(11) Jagadeesh, R. V.; Surkus, A-E.; Junge, H.; Pohl, M-M.; Radnik, J.; Rabeah, J.; Huan, H.; Schünemann, V.; Brückner, A.; Beller, M. Nanoscale Fe_2O_3-based catalysts for selective hydrogenation of nitroarenes to anilines. *Science* **2013**, *342*, 1073-1076.

(12) Miyazaki, M.; Furukawa, S.; Komatsu, T. Regio- and chemoselective hydrogenation of dienes to monoenes governed by a well-structured bimetallic surface. *J. Am. Chem. Soc.* **2017**, *139*, 18231-18239.

(13) Schwob, T.; Kempe, R. A Reusable Co catalyst for the selective hydrogenation of functionalized nitroarenes and the direct synthesis of imines and benzimidazoles from nitroarenes and aldehydes. *Angew. Chem. Int. Ed.* **2016**, *55*, 15175-15179.

(14) Sorribes, I.; Wienhçfer, G.; Vicent, C.; Junge, K.; Llusar, R.; Beller, M. Chemoselective transfer hydrogenation to nitroarenes mediated by cubane-type Mo_3S_4 cluster catalysts. *Angew. Chem.* **2012**, *124*, 1-6.

(15) Ye, T-N.; Xiao, Z.; Li, J.; Gong, Y.; Abe, H.; Niwa, Y.; Sasase, M.; Kitano, M.; Hosono, H.; Stable single platinum atoms trapped in sub-nanometer cavities in $12CaO{\cdot}7Al_2O_3$ for chemoselective hydrogenation of nitroarenes. *Nat. Commun*. **2020**, *11*, 1020.

(16) Furukawa, S.; Takahashi K.; Komatsu, T. Well-structured bimetallic surface capable of molecular recognition for chemoselective nitroarene hydrogenation. *Chem. Sci*. **2016**, *7*, 4476-4484.

(17) Sun, Q.; Wang, N.; Zhang, T.; Bai, R.; Mayoral, A.; Zhang, P.;Q Zhang, Q.; Terasaki, O.; Yu, J. Zeolite-encaged single-atom rhodium catalysts: highly-efficient hydrogen generation and shape-selective tandem hydrogenation of nitroarenes. *Angew. Chem. Int. Ed.* **2019**, *58*, 18570-18576.

(18) Zhang, J.; Wang, L.; Shao, Y.; Wang, Y.; Gates, B. C.; Xiao, F-S.; A Pd@Zeolite catalyst for nitroarene hydrogenation with high product selectivity by sterically controlled adsorption in the zeolite micropores. *Angew. Chem.* **2017**, *129*, 9879-9883.

(19) Liu, Z.; Huang, F.; Peng, M.; Chen, Y.; Cai, X.; Wang, L.; Hu, Z.; Wen, X.; Wang, N.; Xiao, D.; Jiang, H.; Sun, H.; Liu, H.; Ma, D. Tuning the selectivity of catalytic nitriles hydrogenation by structure regulation in atomically dispersed Pd catalysts. *Nat. Commun.* **2021**, *12*, 6194.

(20) Huang, F.; Deng, Y.; Chen, Y.; Cai, X.; Peng, M.; Jia, Z.; Ren, P.; Xiao, D.; Wen, X.; Wang, N.; Liu, H.; Ma, D. Atomically dispersed Pd on nanodiamond/graphene hybrid for selective hydrogenation of acetylene. *J. Am. Chem. Soc.* **2018**, *140*, 13142-13146.

(21) Ma, J.; Mao, X.; Hu, C.; Wang, X.; Gong, W.; Liu, D.; Long, R.; Du, A.; Zhao, H.; Xiong, Y. Highly efficient iron-based catalyst for light-driven selective hydrogenation of nitroarenes. *J. Am. Chem. Soc.* **2024**, *146*, 970-978.

(22) Serna P.; Corma, A. Transforming nano metal nonselective particulates into chemoselective catalysts for hydrogenation of substituted nitrobenzenes. *ACS Catal*. **2015**, *5*, 7114-7121.

(23) Jin, h.; Li, p.; Cui, p.; Shi, j.; Zhou, W.; Yu, X.; Song, W.; Cao, C. Unprecedentedly high activity and selectivity for hydrogenation of nitroarenes with single atomic Co_1-N_3P_1 sites. *Nat. Commun*. **2022**, *13*, 723.

(24) Wei, H.; Liu, X.; Wang, A.; Zhang, L.; Qiao, B.; Yang, X.; Huang, Y.; Miao, S.; Liu, J.; Zhang, T. FeO_x-supported platinum single-atom and pseudo-single-atom catalysts for chemoselective hydrogenation of functionalized nitroarenes. *Nat. Commun*. **2014**, *5*, 5634.

(25) Chan C. W. A.; Mahadi, A. H.; Li, M. M.; Corbos, E. C.; Tang, C.; Jones, G.; Kuo, W. C. H.; Cookson, J.; Brown, C. M.; Bishop, P. T.; Tsang, S. C. E. Interstitial modification of palladium nanoparticles with boron atoms as a green catalyst for selective hydrogenation. *Nat. Commun*. **2014**, *5*, 5787.

(26) Wilson, N. M.; Flaherty, D. W. Mechanism for the direct synthesis of H_2O_2 on Pd clusters: heterolytic reaction pathways at the liquid-solid interface. *J. Am. Chem. Soc.* **2016**, *138*(2), 574-586.

(27) Adams, J. S.; Kromer, M. L.; Rodríguez-López, J.; Flaherty, D. W. Unifying concepts in electro- and thermocatalysis toward hydrogen peroxide production. *J. Am. Chem. Soc.* **2021**, *143*(21), 7940-7957.

(28) Niyazymbetov, M. E.; Evans, D. H. Electrogeneration of the anion of ethyl nitroacetate and its use in electroorganic synthesis. *J. Org. Chem*. **1993**, *58*, 779-783.

(29) Zhou, W.; Li, L.; Qin, R.; Zhu, J.; Liu, S.; Mo, S.; Shi, Z.; Fang, H.; Ruan, P.; Cheng, J.; Fu, G.; Zheng N.; Non-contact biomimetic mechanism for selective hydrogenation of nitroaromatics on heterogeneous metal nanocatalysts. *Sci. China Chem*. **2022**, *65*, 726-732.

(30) An, H.; Sun, G.; Hülsey, M. J.; Sautet, P.; Yan, N. Demonstrating the electron-proton-transfer mechanism of aqueous phase 4-nitrophenol hydrogenation using unbiased electrochemical cells. *ACS Catal.* **2022**, *12*, 15021-15027.

(31) Adams, J. S.; Chemburkar, A.; Priyadarshini, P.; Ricciardulli, T.; Lu, Y.; Maliekkal, V.; Sampath, A.; Winikoff, S.; Karim, A. M.; Neurock, M.; Flaherty, D. W. Solvent molecules form surface redox mediators in situ and cocatalyze O_2 reduction on Pd. *Science* **2021**, *371* (6529), 626-632.

(32) Ryu, J.; Bregante, D. T.; Howland, W. C.; Bisbey, R. P.; Kaminsky, C. J. Surendranath, Y. Thermochemical aerobic oxidation ctalysis in water can be analysed as two coupled electrochemical half-reactions. *Nat. Catal.* **2021**, *4*(9), 742-752.

(33) Chen, G.; Xu, C.; Huang, X.; Ye, J.; Gu, L.; Li, G.; Tang, Z.; Wu, B.; Yang, H.; Zhao, Z.; Zhou, Z.; Fu, G.; Zheng, N. Interfacial electronic efects control the reaction selectivity of platinum catalysts. *Nature Mater*. **2016**, *15*, 564-569.

(34) Zhao, X.; Zhou, L.; Zhang, W.; Hu, C.; Dai, L.; Ren, L.; Wu, B.; Fu, G.; Zheng, N. Thiol treatment creates selective palladium catalysts for semihydrogenation of internal alkynes. *Chem* **2018**, *4*, 1080-1091.

(35) Ruan, P.; Chen, B.; Zhou, Q.; Zhang, H.; Wang, Y.; Liu, K.; Zhou, W.; Qin, R.; Liu, Z.; Fu, G.; Zheng, N. Upgrading heterogeneous Ni catalysts with thiol modification. *The Innovation* **2023**, *4*, 100362.

(36) Wu, Q.; Zhou, W.; Shen, H.; Qin, R.; Hong, Q.; Yi, X.; Zheng, N.; Surface coordination decouples hydrogenation catalysis on supported metal catalysts. *CCS Chem*. **2023**, *5*, 1215-1224.

(37) Chadderdon, X. H.; Chadderdon, D. J.; Matthiesen, J. E.; Qiu, Y.; Carraher, J. M.; Tessonnier, J-P.; Li, W. Mechanisms of furfural reduction on metal electrodes: distinguishing pathways for selective hydrogenation of bioderived oxygenates. *J. Am. Chem. Soc.* **2017**, *139*, 14120-14128.

(38) Marconato, J. C.; Bulhões, L. O.; Temperini, M. L. A spectroelectrochemical study of the inhibition of the electrode process on copper by 2-mercaptobenzothiazole in ethanolic solutions *Electrochim. Acta* **1998**, 43, 771-780 (39)

(39) Woods, R.; Hope, G. A.; Watling, K. J. A SERS spectroelectrochemical investigation of the interaction of 2-mercaptobenzothiazole with copper, silver and gold surfaces *Appl. Electrochem.* **2000**, *30*, 1209-1222.

(40) Hülsey, M. J.; Fung, V.; Hou, X.; Wu, J.; Yan, N. Hydrogen spillover and its relation to hydrogenation: observations on structurally defined single-atom sites. *Angew. Chem*. **2022**, *134*, 1-10.

(41) Wesley, T. S.; Román-Leshkov, Y.; Surendranath, Y. Spontaneous electric fields play a key role in thermochemical catalysis at metal-liquid interfaces. *ACS Cent. Sci.* **2021**, *7*(6), 1045-1055.

(42) Elise M. Miner, E. M.; Fukushima, T.; Sheberla, D.; Sun, L.; Surendranath, Y.; Dinca, M. Electrochemical oxygen reduction catalyzed by Ni_3(hexaiminotriphenylene)$_2$. *Nat. Commun.* **2016**, *7*, 10942.

(43) Gerken, J. B.; McAlpin, J. G.; Chen, J. Y. C.; Rigsby, M. L.; Casey, W. H.; Britt, R. D.; Stahl, S. S. Electrochemical water oxidation with cobalt-based electrocatalysts from pH 0-14: the thermodynamic basis for catalyst structure, stability, and activity. *J. Am. Chem. Soc*. **2011**, *133*, 14431-14442.

(44) Surendranath, Y.; Kanan, M. W.; Nocera, D. G. Mechanistic studies of the oxygen evolution reaction by a cobalt-phosphate catalyst at neutral pH. *J. Am. Chem. Soc.* **2010**, *132*, 16501-16509.

(45) Concepcion, J. J.; Jurss, J. M.; Templeton, J. L.; Meyer, T. J. One Site is enough. Catalytic water oxidation by $[Ru(tpy)(bpm)(OH_2)]^{2+}$ and $[Ru(tpy)(bpz)(OH_2)]^{2+}$. *J. Am. Chem. Soc.* **2008**, *130*, 16462-16463.

(46) Trandafir, M.; Florea, M.; Neat, F.; Primo, A.; Parvulescu, V. I.; Garcia, H. Graphene from alginate pyrolysis as a metal-free catalyst for hydrogenation of nitro compounds. *ChemSusChem* **2016**, *9*, 1565-1569.

(47) Gao, Y.; Ma, D.; Wang, C.; Guan, J.; Bao, X. Reduced graphene oxide as a catalyst for hydrogenation of nitrobenzene at room temperature. *Chem. Commun.* **2011**, *47*, 2432-2434.

(48) Zhao, Z.; Bababrik, R.; Xue, W.; Li, Y.; Briggs, N. M.; Nguyen, D.-T.; Nguyen, U.; Crossley, S. P.;

Wang, S.; Wang, B.; Resasco, D. E. Solvent-mediated charge separation drives alternative hydrogenation path of furanics in liquid water. *Nat. Catal*. **2019**, *2*(5), 431-436.

(49) Shangguan, J.; Chin, Y.; Kinetic significance of proton-electron transfer during condensed phase reduction of carbonyls on transition metal clusters. *ACS Catal.* **2019**, *9*, 1763-1778.

(50) Bates, J.; Biswas, S.; Suh, S.; Johnson, M.; Mondal, B.; Root, T.; Stahl, S. Chemical and electrochemical O_2 reduction on earth-abundant M-N-C catalysts and implications for mediated electrolysis. *J. Am. Chem. Soc.* **2022**, *144*, 922-927.

(51) He, D.; Jiao, X.; Jiang, P.; Wang, J.; Xu, B. An exceptionally active and selective Pt-Au/TiO_2 catalyst for hydrogenation of the nitro group in chloronitrobenzene. *Green Chem*. **2012**, *14*, 111-116.

(52) Shao, J.; Liu, M.; Wang, Z.; Li, K.; Bao, B.; Zhao, S.; Zhou, S. Controllable synthesis of surface Pt-rich bimetallic AuPt nanocatalysts for selective hydrogenation reactions. *ACS Omega* **2019**, *4*, 15621-15627.

(53) Wei, J.; Qin, S.; Liu, J.; Ruan, X.; Guan, Z.; Yan, H.; Wei, D.; Zhang, H.; Cheng, J.; Xu, H.; Tian, Z.; Li, J. In situ raman monitoring and manipulating of interfacial hydrogen spillover by precise fabrication of Au/TiO_2/Pt sandwich structures. *Angew. Chem. Int. Ed.* **2020**, *59*, 10343-10347.

(54) Song, Y.; Wang, H.; Wang, Z.; Guo, B.; Jing, K.; Li, Y.; Wu, L. Selective photocatalytic synthesis of haloanilines from halonitrobenzenes over multifunctional AuPt/monolayer titanate nanosheet. *ACS Catal.* **2018**, *8*, 9656-9664.

(55) Guan, Q.; Zhu, C.; Lin, Y.; Vovk, E.; Zhou, X.; Yang, Y.; Yu, H.; Cao, L.; Wang, H.; Zhang, X.; Liu, X.; Zhang , M.; Wei, S.; Li , W.; Lu, J. Bimetallic monolayer catalyst breaks the activity-selectivity trade-off on metal particle size for efficient chemoselective hydrogenations. *Nat. Catal.* **2021**, *4*, 840-849.

(56) Serna, P.; Concepción, P.; Corma, A. Design of highly active and chemoselective bimetallic gold–platinum hydrogenation catalysts through kinetic and isotopic studies. *J. Catal.* **2009**, *265*, 19-25.

(57) Li, m.; Chen, s.; Jiang, O.; Chen, Q.; Wang, X.; Yan, Y.; Liu, J.; Lv, C.; Ding,W.; Guo, X. Origin of the activity of Co-N-C catalysts for chemoselective hydrogenation of nitroarenes. *ACS Catal.* **2021**, *11*, 3026-3039.

(58) Chen, X.; Shen, K.; Ding, D.; Chen, J.; Fan, T.; Wu, R.; Li, Y. Solvent-driven selectivity control to either anilines or dicyclohexylamines in hydrogenation of nitroarenes over a bifunctional Pd/MIL-101 catalyst. *ACS Catal.* **2018,** *8*, 10641-10648.

Insert Table of Contents artwork here

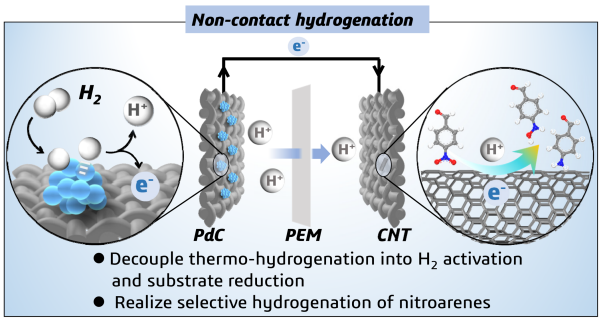
Non-contact hydrogenation
e⁻
H₂
H⁺
e⁻
H⁺
H⁺
H⁺
H⁺
e⁻
PdC
PEM
CNT
● Decouple thermo-hydrogenation into H2 activation and substrate reduction
● Realize selective hydrogenation of nitroarenes